Numerical Investigation of Flow Characteristics Around Bridge Piers with Different Cross-Sectional Geometries

A. Dairi[1], I. Bachir Bouiadjra[2], K. Malti[2], T. Yahiaoui[2] and B. Imine[2]
[1] Department of Hydraulics, Faculty of Architecture and Civil Engineering USTO-MB
[2]Laboratory of Aeronautics and Propulsive Systems, Faculty of Mechanical Engineering,
USTO-MB Oran 31000 Algeria

Abstract

This study numerically investigates the wake flow behind circular, square, triangular, circular corrugated and elliptic cross-sectional geometries under uniform flow conditions using CFD software. The Reynolds-Averaged Navier–Stokes (RANS) turbulence model was employed to simulate the turbulent flow behaviour and evaluate the hydrodynamic characteristics of the studied geometries. Velocity contours, pressure distribution, vortex formation, wake development, and drag coefficients were analysed for each configuration. Particular attention is given to the corrugated pier, whose innovative surface geometry is expected to alter wake dynamics and mitigate flow-induced effects relative to conventional pier configurations. The results show that square, triangular and corrugated piers produce stronger wake disturbances and higher drag coefficients than the circular and elliptic piers due to earlier flow separation and sharp edges. The study provides useful insights into bluff body hydrodynamics and may contribute to the optimization of engineering structures subjected to fluid flow.

Keywords: Bluff body, CFD, Wake flow, Vortex shedding, Drag coefficient, CFD, RANS turbulence model.

1. Introduction

The hydrodynamic behaviour of bluff bodies has been a major research topic in fluid mechanics for several decades because of its importance in civil, mechanical, marine, and aerospace engineering applications. Structures such as bridges, chimneys, cooling towers, offshore platforms, heat exchangers, and tall buildings are continuously exposed to fluid flow interactions that generate complex wake dynamics and vortex shedding phenomena [1].

When a fluid flows around a bluff body, boundary layer separation occurs due to adverse pressure gradients, leading to the formation of alternating vortices downstream of the body. This periodic shedding process forms the well-known Von Kármán vortex street, which may generate fluctuating lift and drag forces responsible for structural vibrations, fatigue damage, and aeroelastic instabilities [2].

Numerous experimental and numerical studies have been conducted to understand the wake flow characteristics behind bluff bodies of different geometries. Roshko [3] carried out pioneering investigations on turbulent wakes and vortex streets behind circular piers, establishing fundamental relationships between Reynolds number and vortex shedding frequency. Later, Williamson [4] provided a comprehensive analysis of vortex dynamics and wake transitions for circular piers over a wide Reynolds number range.

Several researchers investigated the influence of cross-sectional geometry on hydrodynamic performance. Norberg [5] experimentally studied the fluctuating lift forces acting on circular piers and demonstrated the strong dependence of wake instability on Reynolds number. Sohankar et al. [6] numerically analysed the flow around square piers and reported that sharp corners accelerate flow separation and increase wake turbulence intensity compared to circular piers.

Similarly, Okajima [7] investigated the hydrodynamic characteristics of triangular and square piers and showed that sharp-edged bluff bodies generate larger drag coefficients and stronger vortex shedding due to abrupt separation mechanisms. Wang and Zhou [8] examined wake evolution behind triangular piers and observed significant variations in

vortex formation depending on the angle of attack and flow conditions.

With the rapid development of Computational Fluid Dynamics (CFD), numerical simulations have become effective tools for studying bluff body hydrodynamics. CFD approaches provide detailed information about velocity fields, pressure distribution, vortex structures, and hydrodynamic coefficients while reducing experimental costs and time requirements [9]. Among the available numerical methods, the Reynolds-Averaged Navier–Stokes (RANS) approach remains widely used in engineering applications because of its computational efficiency and acceptable prediction accuracy for turbulent external flows [10].

In 2025, several studies have confirmed the importance of pier geometry in the development of turbulent wake flow and local scour. Zhang et al. [11] experimentally demonstrated that the shape and arrangement of piers significantly influence velocity fields and morphological changes of the riverbed. Similarly, Yassin and Al-Shukur [12] highlighted the effect of pier spacing and orientation on the formation of horseshoe vortices and on the evolution of local scour. Furthermore, recent advances in CFD now make it possible to reproduce complex vortex structures around bridge piers with high accuracy. The work of Liang et al. [13], based on Large Eddy Simulation (LES), showed the influence of the number of piers and their spacing on the three-dimensional hydrodynamic characteristics of the wake. Other studies, such as those by Ahmad et al. [14], Zhao et al. [15], and Eini et al. [16], have focused on scour mitigation techniques and on the combined use of CFD and artificial intelligence to improve the prediction of erosion depths around bridge piers. Despite the large number of studies carried out, the comparative influence of different cross-sectional geometries on flow hydrodynamic characteristics remains an open research topic. In this context, the present study aims to numerically investigate the effect of several bridge pier shapes on velocity fields, pressure distribution, turbulent kinetic energy, and wake structure.

The present study numerically investigates the wake flow behind circular, square, triangular, corrugated and elliptic piers subjected to uniform water currents using CFD simulations. Five inlet velocities: 1, 1.5, 2, 2.5, and 3 m/s are considered to evaluate the effect of flow velocity on hydrodynamic behaviour. Particular attention is given to vortex shedding, wake development, velocity distribution, and drag coefficient variations for each pier geometry. The results are used to compare the flow characteristics and hydrodynamic performance of the different configurations under various flow conditions. Special focus is placed on the corrugated pier to assess its ability to modify wake structures and reduce flow-induced effects compared with conventional pier shapes. The findings provide useful information for the design and optimization of bridge piers and other hydraulic structures exposed to river currents.

2. Numerical Methodology

2.1 Geometry Description

Four bluff body geometries were investigated as it shown in figure 1:

- Circular pier
- Square pier
- Triangular pier
- Circular corrugated pier
- Elliptic pier

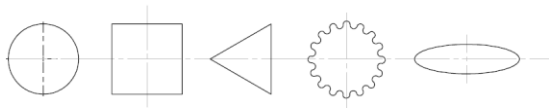

Fig. 1: Different cross-sectional geometries

The study examines five pier cross-sectional geometries—circular, square, triangular, corrugated circular and elliptic—to evaluate the influence of shape on flow behaviour, vortex shedding, wake development, and hydrodynamic forces. The corrugated circular and elliptic piers are a bio-inspired design intended to modify boundary-layer development and mitigate vortex shedding. Together, these geometries enable a comparative assessment of velocity distribution, flow separation, wake characteristics, hydrodynamic loading and local scour processes. All piers were positioned horizontally within a two-

dimensional computational domain under uniform inlet flow conditions.

2.2 Governing Equations

The incompressible turbulent flow is governed by the Reynolds-Averaged Navier–Stokes (RANS) equations with Standard k–ε Turbulence Model [17]:

1. Reynolds Decomposition

$$U_i = \bar{U}_i + u'_i$$
$$P = \bar{P} + p'$$

2. Continuity Equation

$$\partial \bar{U}_i / \partial x_i = 0$$

3. RANS Momentum Equations

$$\rho(\partial \bar{U}_i/\partial t + \bar{U}_j\, \partial \bar{U}_i/\partial x_j) = -\partial \bar{P}/\partial x_i + \mu\, \partial^2 \bar{U}_i/\partial x_j^2 - \rho\, \partial(u'_i u'_j)/\partial x_j$$

4. Boussinesq Hypothesis

$$-\rho u'_i u'_j = \mu_t(\partial \bar{U}_i/\partial x_j + \partial \bar{U}_j/\partial x_i) - 2/3\, \rho k \delta_{ij}$$

2.3 Turbulence Model

The Reynolds-Averaged Navier–Stokes (RANS) turbulence modelling approach was adopted in order to accurately represent the turbulent characteristics of the wake flow. Within this framework, the standard *k–ε* turbulence model was selected because of its proven robustness, numerical stability, and relatively low computational cost. This model is widely used for external hydrodynamic applications involving bluff-body flows, where reliable prediction of mean flow quantities, such as velocity fields, turbulence kinetic energy, and dissipation rate, is required:

Turbulent kinetic energy (k):

$$\partial(\rho k)/\partial t + \partial(\rho U_j\, k)/\partial x_j = \partial/\partial x_j[(\mu + \mu_t/\sigma_k)\, \partial k/\partial x_j] + G_k - \rho\varepsilon$$

Dissipation rate (ε):

$$\partial(\rho\varepsilon)/\partial t + \partial(\rho U_j\, \varepsilon)/\partial x_j = \partial/\partial x_j[(\mu + \mu_t/\sigma_\varepsilon)\, \partial \varepsilon/\partial x_j] + C_{1\varepsilon}\, (\varepsilon/k) G_k - C_{2\varepsilon}\, \rho(\varepsilon^2/k)$$

Turbulent viscosity:

$$\mu_t = \rho\, C_\mu\, k^2 / \varepsilon$$

Standard model constants:

$C_\mu = 0.09$, $C_{1\varepsilon} = 1.44$, $C_{2\varepsilon} = 1.92$, $\sigma_k = 1.0$, $\sigma_\varepsilon = 1.3$

2.4 Boundary Conditions

The following boundary conditions were applied to define the computational domain. A uniform velocity inlet was specified to represent a steady incoming flow. A pressure outlet condition was imposed at the downstream boundary, allowing the flow to leave the domain without significant reflections. The pier surfaces were treated with a no-slip wall condition to accurately capture boundary layer development and flow separation. The upper and lower boundaries were defined as walls, ensuring flow confinement and numerical stability throughout the simulations.

2.5 Numerical Solver

CFD software was employed to perform the numerical simulations of the flow field [18]. A pressure-based solver was selected as it is particularly suitable for incompressible or low-Mach-number flows commonly encountered in external hydrodynamic applications. This solver formulation ensures a strong coupling between pressure and velocity fields, which is essential for accurately resolving wake dynamics and vortex shedding phenomena. To enhance the accuracy of the numerical results, second-order discretization schemes were applied for the spatial derivatives in both momentum and turbulence transport equations. Compared to first-order schemes, the second-order approach significantly reduces numerical diffusion and provides improved resolution of steep gradients in velocity, pressure, and turbulence quantities. This leads to a more precise prediction of flow separation, wake development, and unsteady flow structures around the bluff bodies considered in the study.

3. Results and Discussion

This study employs Computational Fluid Dynamics (CFD) to investigate the wake flow characteristics around circular, square, triangular, corrugated and elliptic piers exposed to uniform water currents. To examine the influence of flow velocity on hydrodynamic behaviour, simulations are carried out for five inlet velocities ranging from 1 to 3 m/s (1, 1.5, 2, 2.5, and 3 m/s).

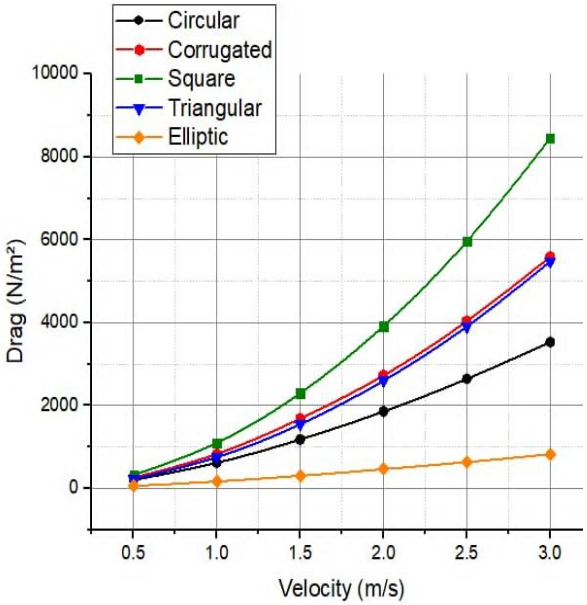

Fig.3 : Variation of drag force as a function of flow velocity

The figure 3 shows the variation of drag force with flow velocity for five pier geometries: circular, corrugated circular, square, triangular, and elliptical. For all configurations, the drag force increases as the flow velocity increases. The square pier produces the highest drag values, reaching approximately 8400 N/m² at 3 m/s due to strong flow separation and wake formation. The corrugated and triangular piers exhibit intermediate behavior, with drag forces around 5500–5600 N/m² at the highest velocity. The circular pier generates lower drag values, reaching about 3500 N/m² at 3 m/s. The elliptical pier demonstrates the best hydrodynamic performance, with the lowest drag force throughout the investigated velocity range, reaching only about 800 N/m² at 3 m/s. This reduction is attributed to its streamlined shape, which delays flow separation and weakens the downstream wake. Overall, the results indicate that the elliptical geometry is the most effective in reducing hydrodynamic loads and may contribute to mitigating local scour around bridge foundations.

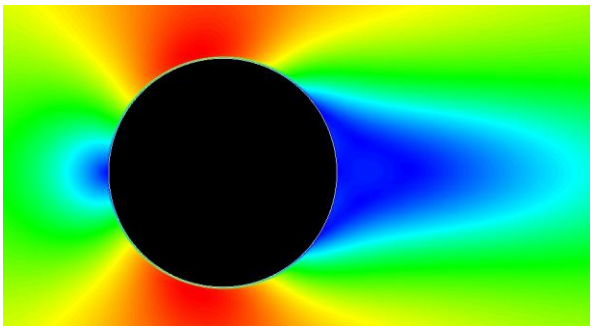

Fig. 4: Velocity magnitude contours of a river flow around a circular-section bridge pier

Contours of velocity magnitude around a circular pier are shown in Figure 4. The flow moves from left to right and interacts with the pier, creating a stagnation region at the front where the velocity decreases significantly. As the fluid flows around the pier, it accelerates along the upper and lower surfaces, reaching its maximum values in the red regions. Downstream of the pier, a low-velocity wake develops due to flow separation, as indicated by the blue region behind the body. The velocity gradually recovers further downstream as the flow re-establishes itself. This wake region is associated with momentum losses and contributes significantly to the drag acting on the pier.

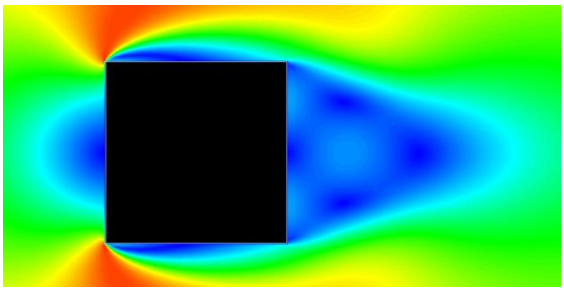

Fig. 5: Velocity magnitude contours of a river flow around a square-section bridge pier

The figure 5 illustrates the velocity magnitude contours of a river flow interacting with a square-section bridge pier. The water flows from left to right and encounters the obstacle, causing significant modifications to the local flow field. Upstream of the pier, a stagnation

zone develops on the front face where the incoming flow impinges directly on the structure. In this region, the flow velocity decreases sharply while the pressure reaches its maximum value. As the water moves around the sharp corners of the pier, the flow accelerates, generating high-velocity regions near the upper and lower leading edges. Downstream of the pier, the flow separates abruptly from the rear corners due to the sudden geometric discontinuity. This separation creates a wake region characterized by low velocities and flow recirculation. The wake contains a series of vortex structures, indicating the development of unsteady flow instabilities and periodic vortex shedding. These vortices are responsible for the oscillatory behaviour commonly observed behind bluff bodies immersed in open-channel flows. From a hydraulic engineering perspective, the presence of the pier induces energy losses and generates significant hydrodynamic forces on the structure. The alternating vortices produce fluctuating pressure loads that may contribute to structural vibrations. Furthermore, the highly turbulent flow in the wake region can increase bed shear stresses around the base of the pier, potentially leading to local scour and sediment erosion. Overall, the figure clearly demonstrates the main flow phenomena associated with a square bridge pier in a river environment: flow stagnation upstream, acceleration around the side edges, flow separation at the rear corners, and the formation of a turbulent wake with recirculating vortices downstream. These features are of primary importance in the design and assessment of hydraulic structures subjected to river currents.

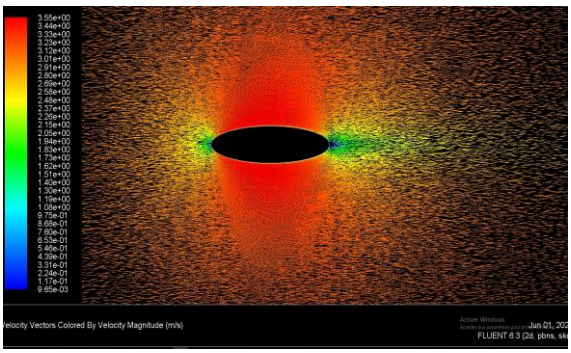

Fig. 7: Contours of velocity vector for elliptical pier

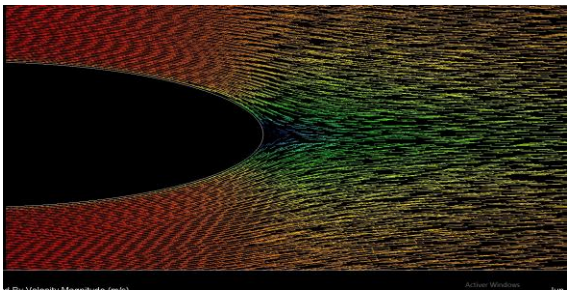

Fig. 8: Detail of Contours of velocity vector for elliptical pier

The figure 8 shows the velocity contours and flow vectors around an elliptical pier subjected to a uniform flow. A stagnation zone is observed at the upstream face of the pier, where the velocity decreases significantly. As the flow moves around the upper and lower surfaces, it accelerates due to the streamlined shape of the ellipse, leading to higher velocity regions near the sides. Downstream of the pier, a relatively narrow wake with reduced velocity is formed. The elliptical geometry delays flow separation and limits the development of large recirculation zones, resulting in a smoother wake and lower turbulence intensity. Overall, the streamlined shape promotes better flow recovery and reduces hydrodynamic drag compared with bluff-body geometries.

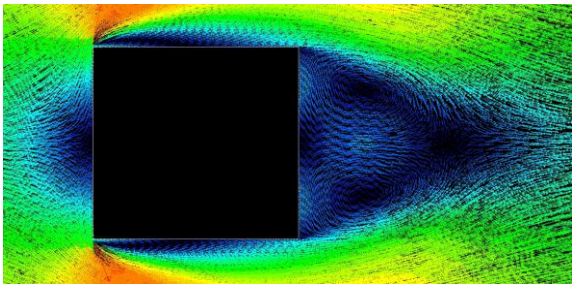

Fig. 10 : Velocity Vectors Contours for square bridge pier for V = 3 m/s

This figure 10 illustrates the flow field around a square pier subjected to a uniform flow, represented both by streamlines and the velocity distribution (colour scale). A clear stagnation point is observed at the upstream leading edge of the pier, where the fluid velocity becomes nearly zero due to the direct impingement of the incoming flow on the front face. As the fluid flows around the obstacle, it undergoes significant acceleration along the side faces, as indicated by the warm-colored regions (yellow to red), which correspond to high-velocity zones. This acceleration is associated with the local reduction in effective flow area and the deflection of the streamlines

around the geometry. Downstream of the pier, a wake region is clearly visible, characterized by strong flow deceleration and flow separation. Two symmetric recirculation structures develop in the downstream region, indicating the formation of a wake typical of bluff bodies. These recirculation zones are associated with high velocity gradients and wake instability, which are precursors to vortex shedding phenomena. Overall, the figure highlights the early boundary layer separation at the sharp edges of the square pier, the formation of an extended downstream wake, and the pronounced local asymmetry in the velocity field, all of which are classical features of flow around sharp-edged geometries.

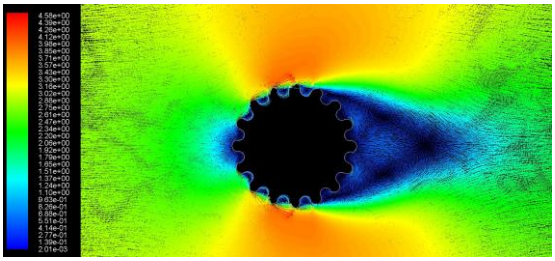

Fig.11: Velocity contour around a corrugated circular bridge pier case for a velocity V = 3 m/s

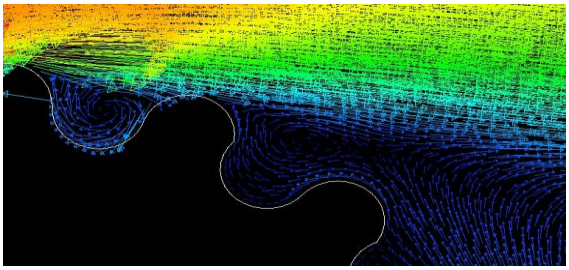

Fig.12 : Small recirculation zones within the cavities

Figure 11 shows the instantaneous velocity field around a corrugated circular cross-section obtained from numerical simulations. The coloured contours represent the velocity magnitude, while the velocity vectors illustrate the overall flow pattern. Upstream of the post, the flow remains uniform with an almost constant velocity. At the front of the obstacle, a stagnation region is observed where the velocity decreases to nearly zero. As the flow moves around the post, it accelerates along the upper and lower sides, leading to higher velocity regions shown in orange and red. As it shown in figure 12 , the surface undulations affect the boundary-layer behaviour by generating small recirculation zones within the cavities of the post. These local vortices enhance momentum exchange near the wall and influence the flow separation process. Downstream of the post, flow separation occurs and forms a wake region characterized by low velocities, visible in blue. Several vortical structures can be observed within the wake, indicating unsteady flow behaviour and energy dissipation. The wake size and vortex intensity are closely related to the drag acting on the obstacle. Overall, the results demonstrate that the surface undulations have a significant effect on the flow structure, particularly on boundary-layer development, flow separation, and wake formation. Understanding these effects is important for improving the hydrodynamic performance of cylindrical structures and reducing drag forces.

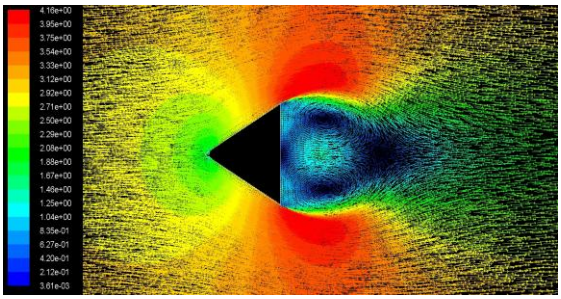

Fig.13: Velocity contour around a triangular bridge pier for a velocity V = 3 m/s

Figure 13 shows the velocity vector around the studied obstacle under a uniform incoming flow. A stagnation region is observed at the front face of the obstacle, where the fluid velocity decreases significantly due to the direct impact of the flow. As the fluid passes around the obstacle, it splits into two streams and accelerates along the upper and lower surfaces, producing high-velocity regions indicated by the red contours. Behind the obstacle, flow separation occurs at the sharp rear edges, leading to the formation of a wake characterized by low velocity values (blue region). The velocity vector contours clearly reveal two counter-rotating recirculation zones in the near-wake region, which are typical of bluff-body flows. These vortical structures result from the adverse pressure gradient and the inability of the flow to remain attached to the obstacle surface.

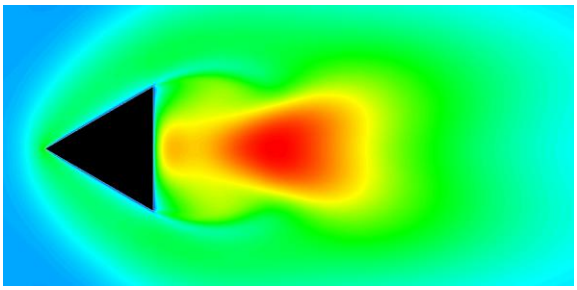

Fig. 6: Distribution of turbulent kinetic energy **(k)** around a triangular bridge pier

This figure 6 shows the distribution of turbulent kinetic energy (k) around a triangular obstacle. The colour scale ranges from low values (blue) to high values (red). Upstream of the obstacle, the turbulent kinetic energy is low, indicating a relatively stable flow. As the fluid passes around the sharp edges of the triangle, turbulence is generated and the value of turbulent kinetic energy increases. The highest turbulent kinetic energy is observed in the wake region behind the obstacle (red zone). This is caused by flow separation and strong mixing of the fluid. Further downstream, the turbulent kinetic energy gradually decreases as the turbulence dissipates and the flow starts to recover. Overall, the figure highlights the formation of a turbulent wake behind the triangular obstacle, with the maximum turbulence occurring just downstream of the body.

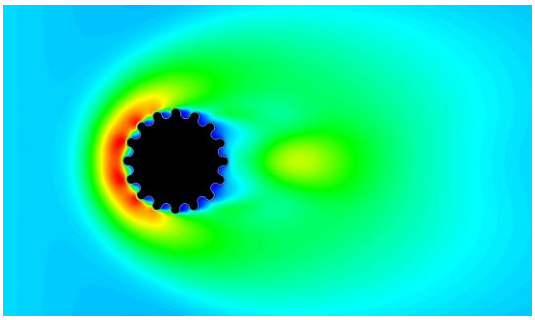

Fig.6 : Contours of turbulent kinetic energy around a corrugated circular pier

The figure 6 shows the distribution of turbulent kinetic energy (k) around a corrugated circular pier subjected to water flow. Upstream of the pier, low TKE values are observed, indicating a relatively uniform flow with weak turbulence. As the fluid approaches the obstacle, flow acceleration along the pier surface generates strong velocity gradients, leading to a significant increase in turbulent kinetic energy. The highest values, reaching approximately 1.95 m^2/s^2, are located on both sides of the pier.

The corrugated geometry promotes local flow separation and the formation of small vortical structures near the surface, which enhances turbulence production. In the near wake region, a low-TKE zone appears behind the pier, corresponding to a recirculation region caused by flow separation. Further downstream, TKE increases again as vortices develop and transport turbulent energy into the wake.

The asymmetric distribution of turbulent kinetic energy in the wake suggests alternating vortex shedding, a typical feature of high-Reynolds-number flows around bluff bodies. Overall, the results indicate that the corrugated circular pier significantly modifies the flow structure and enhances turbulence generation in its vicinity.

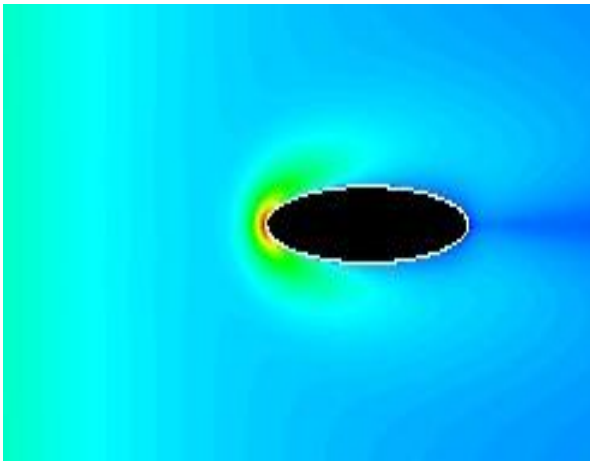

Fig. 9: contours of the turbulent kinetic energy around an elliptical bridge pier

The figure 9 illustrates the contours of the turbulent kinetic energy (k) around an elliptical pier subjected to a uniform water flow. The highest turbulence levels are observed near the upstream face of the obstacle, where the velocity gradients are the strongest. The flow then distributes symmetrically around the pier, leading to a gradual decrease in **k** along the surface of the ellipse. Downstream, the presence of a turbulent wake reflects the shear and mixing phenomena generated as the flow passes around the obstacle. The symmetry of the contours indicates a stable flow with no significant angle of attack, while the elliptical geometry promotes a reduction in turbulence intensity within the wake compared to bluffer

shapes. This distribution highlights the mechanisms of production, transport, and dissipation of turbulent kinetic energy in the flow around the pier.

4- Conclusion

This study numerically investigated the flow behaviour around circular, square, triangular, corrugated and elliptic piers subjected to uniform incoming flow conditions using CFD simulations. The results revealed that pier geometry plays a crucial role in determining flow separation, vortex shedding, wake development, pressure distribution, and hydrodynamic forces.

The square pier generated the largest wake and strongest flow disturbances due to early flow separation, whereas the triangular pier exhibited a more streamlined behaviour with reduced wake intensity. The circular pier served as a useful reference case, displaying the classical vortex shedding pattern. The corrugated pier showed a noticeable modification of the wake structure and a reduction in flow instabilities, highlighting the potential of bio-inspired geometries for flow control applications.

Overall, the findings demonstrate that geometric optimization can significantly improve the hydrodynamic performance of structures exposed to water currents. These results provide valuable insights for the design of bridge piers and other hydraulic structures, with the objective of reducing drag forces, mitigating vortex-induced vibrations, and minimizing local scour. Future work should focus on three-dimensional simulations and experimental validation to further assess the effectiveness of corrugated geometries under realistic flow conditions.

References

[1] Zdravkovich, M.M., Flow Around Circular Piers, Oxford University Press, 1997.

[2] Blevins, R.D., Flow-Induced Vibration, Van Nostrand Reinhold, 1990.

[3] Roshko, A., “On the Development of Turbulent Wakes from Vortex Streets,” NACA Report 1191, 1954.

[4] Williamson, C.H.K., “Vortex Dynamics in the Pier Wake,” Annual Review of Fluid Mechanics, Vol. 28, 1996, pp. 477–539.

[5] Norberg, C., “Flow Around a Circular Pier: Aspects of Fluctuating Lift,” Journal of Fluids and Structures, Vol. 15, 2001, pp. 459–469.

[6] Sohankar, A., Norberg, C., and Davidson, L., “Numerical Simulation of Unsteady Flow Around a Square Two-Dimensional Pier,” Physics of Fluids, Vol. 11, No. 2, 1999, pp. 288–306.

[7] Okajima, A., “Strouhal Numbers of Square Piers,” Journal of Fluid Mechanics, Vol. 123, 1982, pp. 379–398.

[8] Wang, H.F., and Zhou, Y., “The Effects of Angle of Attack on Vortex Shedding from a Triangular Pier,” Journal of Fluids and Structures, Vol. 23, 2007, pp. 413–431.

[9] Versteeg, H.K., and Malalasekera, W., An Introduction to Computational Fluid Dynamics: The Finite Volume Method, Pearson Education, 2007.

[10] Anderson, J.D., Computational Fluid Dynamics: The Basics with Applications, McGraw- Hill, 1995.

[11] Zhang, Y., Chen, B., Wang, S., & Zhang, X. (2025). Physical Model Research on the Impact of Bridge Piers on River Flow in Parallel Bridge Construction Projects. Applied Sciences, 15(12), 6581. https://doi.org/10.3390/app15126581

[12] Yassin, H. A., & Al-Shukur, A. H. K. (2025). Effect of Spacing and Skewness on Side-by-Side Bridge Piers. Mathematical Modelling of Engineering Problems, 12(4), 1150–1158. https://doi.org/10.18280/mmep.120406

[13] Liang, W., Chen, X., Tang, L., Zhang, J., & Cheng, J. (2025). Three-Dimensional Large Eddy Simulation of Hydrodynamics in Multi-Pier Tandem Bridge Systems.

Scientific Reports, 16, 4188. https://doi.org/10.1038/s41598-025-34259-x

[14] Ahmad, A., Khan, M., Ajmal, M., Sher, S., Waseem, M., & Baig, F. (2025). Potential of Roughening Geometric Elements as Bridge Pier Local Scour Countermeasures. Scientific Reports, 15, 8000. https://doi.org/10.1038/s41598-025-92410-0

[15] Zhao et al. (2025). Study on the Mechanism of Local Scour Around Bridge Piers. Journal of Marine Science and Engineering, 13(6), 1021. https://doi.org/10.3390/jmse13061021

[16] Eini, N., Janizadeh, S., Bateni, S. M., Jun, C., & Heggy, E. (2025). Scour depth estimation using standalone metaheuristic algorithms and their combinations with CatBoost. *Scientific* Reports**,** 15, 37239. DOI: 10.1038/s41598-025-21120-4.

[17] Launder, B.E., & Spalding, D.B. (1974). The Numerical Computation of Turbulent Flows. Computer Methods in Applied Mechanics and Engineering, 3(2), 269–289.

[18] Versteeg, H.K., & Malalasekera, W. (2007). An Introduction to Computational Fluid Dynamics: The Finite Volume Method (2nd ed.). Pearson Education.